Progress In Electromagnetics Research C, Vol. 134, 39–52, 2023

Synthesis of Linear Antenna Array for Wireless Power Transmission

Hua Guo*, Jiajie Li, Huiliang Hao, Peng Song, Lijian Zhang, and Xiaodan Zhang

Abstract—A new synthesis method of linear array antenna for wireless power transmission is introduced based on invasive weed algorithm in this paper. In order to improve the beam collection efficiency, the subarray division is carried out in the case of different azimuth angles and different numbers of array elements, respectively. Under the constraints of aperture size and minimum element spacing, the element positions, excitation coefficients, and the element numbers of subarrays are optimized simultaneously. Compared with the optimization results obtained by other literature, it can be found that the proposed method in this paper can obtain a higher beam collection efficiency.

1. INTRODUCTION

Wireless power transmission (WPT) has widespread application in many fields currently [1, 2]. For example, powering unmanned aerial vehicle (UAV) [3] and supplying energy to remote areas. Additionally, space solar power station (SSPS) is also an important application for long-range wireless power transmission [4–8]. Transmitting antenna and receiving antenna are two key components of a WPT system. Transmitting antenna is used to concentrate the radiated power to the receiving antenna while receiving antenna is used to collect microwave power and convert it to direct-current (DC) power [9, 10]. As a power transmission system, its transmission efficiency is vital. Although the total efficiency of a WPT system is influenced by many factors, beam collection efficiency (BCE) appears particularly important.

The meaning of BCE is the ratio of the microwave power captured by the receiving antenna to the total power radiated by the transmitting antenna. Excellent array performance is necessary to satisfy the demands of WPT system, and the system cost should be minimized. Synthesis techniques have been proposed for accomplishing both of these objectives, including stochastic approaches [11–13] and subarray division technique [14–17]. Besides, the maximum BCE and the corresponding excitation coefficients of a linear or planar antenna array can be obtained by solving the maximum generalized eigenvalues and eigenvectors of the matrix [18, 19]. However, the synthesized antenna array is complex and expensive because each array element requires an amplifier. The subarray division of array antennas is to divide the whole antenna array into multiple subarrays. Based on this method, the number of amplifiers required equals the number of subarrays. Therefore, the subarray division technique has a wide range of applications in the design of antenna arrays. In addition, many swarm intelligence optimization algorithms, such as genetic algorithm (GA), particle swarm optimization (PSO), and brainstorming optimization (BSO) [20], are applied to this field. In [20], an improved PSO algorithm was used to optimize planar arrays, and GA and BSO were applied to optimize linear arrays in [21]. Although the results obtained have been improved, the above algorithms have disadvantages such as complex implementation, small search space, and low precision. Invasive weed optimization (IWO) is an emerging swarm intelligence optimization algorithm that was proposed by Mehrabian and Lucas in 2006 [22]. With the larger search space and better robustness than above algorithms, the IWO algorithm

Received 8 March 2023, Accepted 10 June 2023, Scheduled 27 June 2023

* Corresponding author: Hua Guo (xdguohua@163.com).

The authors are with the School of Electronics and Information, Xi'an Polytechnic University, Xi'an 710048, China.

has been successfully applied in many fields. Additionally, the study proves that sparse arrays are more flexible and less costly than thinned arrays [23–25]. Therefore, the optimization problem of sparse array will also be studied in this paper.

A new synthesis method for linear array under the multiple constraints of element numbers, azimuth angles, aperture size, and minimum element spacing is proposed based on the IWO algorithm in this paper. The outline of this paper is as follows. The mathematical model and synthesis methods are given in Section 2. In Section 3, the numerical analysis and discussion are provided. Finally, the conclusion is drawn in Section 4.

2. MATHEMATICAL MODELS AND SYNTHESIS METHODS

2.1. Optimization Process of Odd Array Elements

2.1.1. Array Structure

The geometry of the nonuniform symmetric linear array when the number of array elements is odd is shown in Fig. 1.

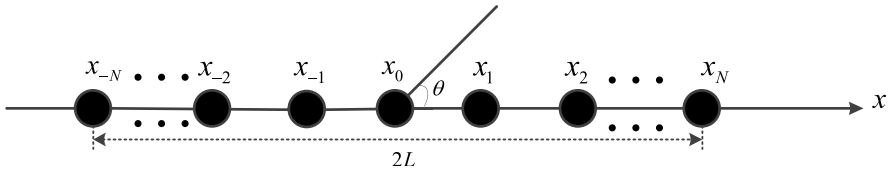

Figure 1. Linear array structure of odd array elements.

From Fig. 1, it can be found that $2N + 1$ array elements are arranged in a straight line, and the aperture size is $2L$. One array element is placed at the coordinate origin, and others are placed symmetrically about the origin of the coordinates, i.e., $x_0 = 0$, $x_n = x_{-n}$, $n = 1, 2, \cdots, N$. The array factor can be expressed as

$$F(u) = I_0 + 2\sum_{n=1}^{N} I_n \cos(kx_n u) \tag{1}$$

where I_n and x_n denote the excitation amplitude and coordinate of the nth array element, respectively. The wavelength is depicted by λ, and the wave number is given by $k = 2\pi/\lambda$. $u = \cos\theta$, θ is the azimuth angle between transmitting antenna and receiving area, $0 \le \theta \le \pi$. Assuming that the array elements are uniformly excited, i.e., $I_n = 1$, the far-field power pattern can be expressed as

$$P(u) = |F(u)|^2 = \left[I_0 + 2\sum_{n=1}^{N} I_n \cos(kx_n u)\right]^2 \tag{2}$$

According to the definition of BCE, it can be expressed as

$$BCE = \frac{P_\psi}{P_\Omega} = \frac{\int_\psi P(u)du}{\int_\Omega P(u)du} \tag{3}$$

where P_ψ and P_Ω denote the power received through azimuth ψ and the total power emitted in the field of view Ω, respectively.

If the maximum BCE is obtained only by optimizing element positions, the optimization model can be expressed as

$$\begin{cases} find\ \mathbf{X} = (x_1, x_2, \cdots, x_{N-1}) \\ \min . f(\mathbf{X}) = -BCE \\ s.t.\ x_i - x_j \ge d_e,\ 0 \le j < i \le N \\ x_0 = 0,\ x_N = L \end{cases} \tag{4}$$

where $\mathbf{X} = (x_1, x_2, \cdots, x_{N-1})$ denotes the coordinates of the best element positions that maximizes the BCE. The fitness function $f(\mathbf{X})$ is $-$BCE which is used to convert the optimization problem into a standard minimization problem. In order to reduce the mutual coupling effect between the array elements, the minimum spacing of any two array elements should satisfy a certain constraint. In this paper, d_e is set to the minimum spacing of the adjacent array elements.

2.1.2. Optimization Method

If the total number of array elements is odd, there are $N+1$ array elements randomly distributed in the right half aperture. The coordinates of the first and last array elements are determined as (0, 0) and (L, 0), respectively. Therefore, the element numbers to be optimized are $N-1$. If all array elements are uniformly arranged according to the minimum element spacing, the length that can be optimized is given by

$$SL = L - Nd_e \tag{5}$$

Then, $N-1$ random numbers that among the rang of [0, SL] can be obtained by

$$s_i' = SL \times z_i,\ i = 1, 2, \cdots, N-1 \tag{6}$$

where z_i is the optimization variable belonging to [0, 1]. $\mathbf{S} = [s_1, s_2, \cdots, s_{N-1}]^T$ is a new random vector obtained by arranging s_i' from smallest to largest, where $s_1 \leq s_2 \leq, \cdots, \leq s_{N-1}$. In this case, the final element positions can be calculated by

$$\begin{bmatrix} x_1 \\ x_2 \\ \cdots \\ x_{N-1} \end{bmatrix} = \mathbf{S} + \begin{bmatrix} d_e \\ 2d_e \\ \cdots \\ (N-1)d_e \end{bmatrix} = \begin{bmatrix} s_1 + d_e \\ s_2 + 2d_e \\ \cdots \\ s_{N-1} + (N-1)d_e \end{bmatrix} \tag{7}$$

2.2. Optimization Process of Even Array Elements

2.2.1. Array Structure

The geometry of the nonuniform symmetric linear array when the number of array elements is even is shown in Fig. 2.

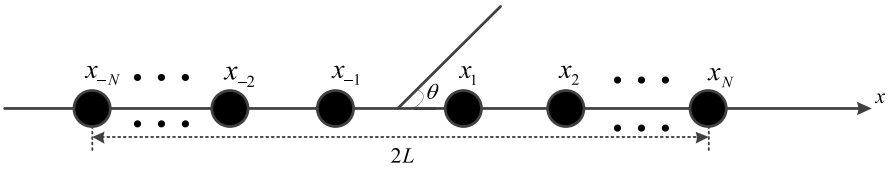

Figure 2. Linear array structure of even array elements.

It can be found that there are $2N$ array elements in a straight line, and the aperture size is $2L$. The array elements are also symmetrically distributed about the coordinate origin. In this case, the array factor can be rewritten as

$$F(u) = 2\sum_{n=1}^{N} I_n \cos(kx_n u) \tag{8}$$

Accordingly, the far-field power pattern can be rewritten as

$$P(u) = |F(u)|^2 = \left[2\sum_{n=1}^{N} I_n \cos(kx_n u)\right]^2 \tag{9}$$

Similarly, if the maximum BCE is obtained only by optimizing the element positions, the optimization model in the case of even array elements can be rewritten as

$$\begin{cases} find\ \mathbf{X} = (x_1, x_2, \cdots, x_{N-1}) \\ \min . f(\mathbf{X}) = -BCE \\ s.t. x_i - x_j \geq d_e,\ 0 < j < i \leq N \\ x_N = L \end{cases} \tag{10}$$

2.2.2. Optimization Method

If the total number of array elements is even, only N array elements are randomly distributed in the right half aperture. The coordinate of the last array element is determined as (L, 0). Therefore, the element numbers to be optimized are also $N-1$. If all array elements are uniformly arranged according to the minimum element spacing, the length that can be optimized is given by

$$SL = L - (N - 0.5)d_e \tag{11}$$

Then, $N-1$ random numbers that in the range of [0, SL] can be obtained by

$$s_i' = SL \times z_i, i = 1, 2, \cdots, N-1 \tag{12}$$

where z_i is also the optimization variable belong to [0, 1]. $\mathbf{S} = [s_1, s_2, \cdots, s_{N-1}]^T$ is a new random vector obtained by arranging s_i' from the smallest to largest, where $s_1 \leq s_2 \leq, \cdots, \leq s_{N-1}$. In this case, the final element positions can be calculated by

$$\begin{bmatrix} x_1 \\ x_2 \\ \cdots \\ x_{N-1} \end{bmatrix} = \mathbf{S} + \begin{bmatrix} 0.5d_e \\ 1.5d_e \\ \cdots \\ (N-1.5)d_e \end{bmatrix} = \begin{bmatrix} s_1 + 0.5d_e \\ s_2 + 1.5d_e \\ \cdots \\ s_{N-1} + (N-1.5)d_e \end{bmatrix} \tag{13}$$

2.3. Optimization Process for Subarray

2.3.1. Subarray Structure

In order to reduce the design complexity and cost of the system, a new optimization method is proposed in this subsection that is subarray division of linear arrays. The subarray structure is shown in Fig. 3. The array elements at the coordinate origin do not participate in the subarray division. So, the element numbers to be optimized in the half-aperture is always N.

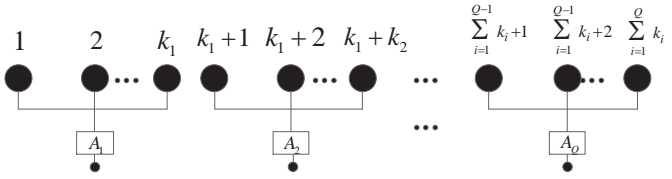

Figure 3. Subarray structure of the linear array.

It is clear that right half of the linear array is divided into Q subarrays. The excitation coefficients and the element numbers of subarrays are A_q and k_q, respectively, $q = 1, 2, \cdots, Q$. The excitation coefficient of each subarray is different, but the excitation amplitude of array elements is the same in the same subarray. The relationship between the excitation amplitude of each array element and the excitation coefficient of each subarray can be expressed as

$$I_n = \sum_{q=1}^{Q} \delta_{s_n q} A_q, \quad n = 1, 2, \cdots, N \tag{14}$$

where $s_n \in [1, Q]$ is a positive integer that denotes the serial number of the subarray to which the nth array element belongs. $\delta_{s_n q}$ is the Dirac function which can be given by

$$\delta_{s_n q} = \begin{cases} 1, & if\ s_n = q \\ 0, & else \end{cases} \tag{15}$$

Then, bring Equation (14) into Equations (1) and (8). In the case of odd and even array elements, the array factor can be represented as

$$F(u) = I_0 + 2\sum_{q=1}^{Q} A_q \sum_{n=1}^{N} \delta_{s_n q} \cos(k x_n u) \tag{16}$$

$$F(u) = 2\sum_{q=1}^{Q} A_q \sum_{n=1}^{N} \delta_{s_n q} \cos(k x_n u) \tag{17}$$

Accordingly, the far-field power pattern can be represented as

$$P(u) = |F(u)|^2 = \left[I_0 + 2\sum_{q=1}^{Q} A_q \sum_{n=1}^{N} \delta_{s_n q} \cos(k x_n u) \right]^2 \tag{18}$$

$$P(u) = |F(u)|^2 = \left[2\sum_{q=1}^{Q} A_q \sum_{n=1}^{N} \delta_{s_n q} \cos(k x_n u) \right]^2 \tag{19}$$

Obviously, the excitation coefficients and the element numbers of subarrays also need to be optimized in the case of subarray division. Therefore, the optimization model can be expressed as

$$\begin{cases} find\ \mathbf{X} = (x_1, \cdots, x_{N-1}, A_2, \cdots, A_q, k_1, \cdots, k_{Q-1}) \\ \min . f(\mathbf{X}) = -BCE \\ s.t.\ x_i - x_j \geq d_e,\ 0 < j < i \leq N \\ \quad 0 < A_q \leq 1,\ q = 2, 3, \cdots, Q \\ \quad K_{\min} \leq k_{\mathrm{q}} \leq K_{\max},\ q = 1, 2, \cdots, Q-1 \\ \quad k_Q = N - \sum_{q=1}^{Q-1} k_q \end{cases} \tag{20}$$

where $\mathbf{X} = (x_1, \cdots, x_{N-1}, A_2, \cdots, A_q, k_1, \cdots k_{Q-1})$ denotes the parameters to be optimized. The minimum and maximum element numbers of subarrays are $K_{\min}$ and $K_{\max}$, respectively, where $K_{\min} \geq 1$ and $K_{\max} \leq N - (Q-1) \times K_{\min}$.

2.3.2. Optimization Method

In Equation (20), the first $N-1$ elements of the vector $\mathbf{X}$ are the element positions, which is optimized in the same way as the above two cases.

Then, the following $Q-1$ elements of the vector $\mathbf{X}$ are the excitation coefficients of subarrays. Since the excitation coefficients are random numbers that in the range of [0, 1], it can be expressed as

$$A_i = 1 \times z_i, i = N, N+1, \cdots, Q+N-2 \tag{21}$$

where z_i is still the optimized variable, and A_i is the excitation coefficient of each subarray.

Finally, the last $Q-1$ elements of the vector $\mathbf{X}$ are element numbers of subarrays. Assuming that the element number of each subarray is $K_{\min}$, then the remaining element numbers available for optimization can be expressed as

$$K_s = N - Q \times K_{\min} \tag{22}$$

$\mathbf{M}_s$ is defined as a new vector, and the element in $\mathbf{M}_s$ can be determined by

$$\begin{cases} M_s(1) = 0 \\ M_s(q) = round(-0.49 + (K_s + 0.98) \times z_{N+Q+q-3}) \end{cases}, \quad q = 2, 3, \cdots, Q \tag{23}$$

where *round* denotes the rounding function. A new vector $\mathbf{M}$ obtained by arranging the elements in $\mathbf{M_s}$ from the smallest to largest, i.e., $M(1) \leq M(2) \leq \cdots \leq M(Q)$. $M(q) \in [0, K_s]$ denotes the total element numbers of the previous $Q-1$ subarrays after subtracting the minimum elements numbers from each subarray. Its mathematical expression can be expressed as

$$\begin{cases} M(1) = 0 \\ M(q) = \sum_{i=1}^{q-1} (k_i - K_{\min}) \end{cases}, \quad q = 2, 3, \cdots, Q \tag{24}$$

The final element numbers of subarrays can be expressed as

$$\begin{cases} k_q = K_{\min} + [M(q+1) - M(q)] \\ k_Q = N - \sum_{q=1}^{Q-1} k_q \end{cases}, \quad q = 1, 2, \cdots, Q-1 \tag{25}$$

2.3.3. Optimization Step

The IWO algorithm mimics the evolutionary principles of weeds in nature to select the best individuals. The specific optimization steps to achieve subarray division of linear array by using IWO algorithm are as follows.

Step 1: A $(2Q + N - 3) \times P$ matrix $\mathbf{z}$ in the range of $[0, 1]$ is generated as the initial population, and the matrix $\mathbf{z}$ is depicted by $\mathbf{z} = [\mathbf{z}^1, \mathbf{z}^2, \cdots, \mathbf{z}^p]$ and $\mathbf{z}^p = [\mathbf{z}_1^p, \mathbf{z}_2^p, \cdots, \mathbf{z}_{2Q+N-3}^p]^T$. The element of matrix $\mathbf{z}$ is given by $z_i^p \in [0, 1]$, i=$1, 2, \cdots, 2Q + N - 3, p = 1, 2, \cdots, P$.

Step 2: The element positions are calculated by Equations (7) or (13). The excitation coefficients and the element numbers of subarrays are calculated by (21) and (25), respectively.

Step 3: The power pattern can be calculated by Equation (16) or (17). The maximum BCE is determined by Equation (3). The fitness function is determined by Equation (20).

Step 4: Update the optimization variable $\mathbf{z}^p$ by IWO algorithm.

Step 5: Let $iter = iter + 1$, if $iter < iter\_\max$, return to Step 2. Otherwise, terminate the iteration and output the result.

In order to describe the algorithm more clearly, the optimization process of the used algorithm is given in Fig. 4.

3. NUMERICAL ANALYSIS AND DISCUSSION

In this section, the arithmetic example from [21] is selected for optimal design. In order to verify the effectiveness and feasibility of used algorithm and proposed method, the parameters are all consistent with the simulation arithmetic examples in [21]. All simulations were computed in MATLAB R2019a with a computer configuration of i5-6500 CPU, 8 GB RAM. The parameters of the IWO are shown in Table 1.

Table 1. The parameters of IWO.

Parameter	$iter\_\max$	P_MAX	$S_{\max}$	$S_{\min}$	n	P	$\sigma_{\max}$	$\sigma_{\min}$
Values	500	30	12	1	3	10	0.1	1e-4

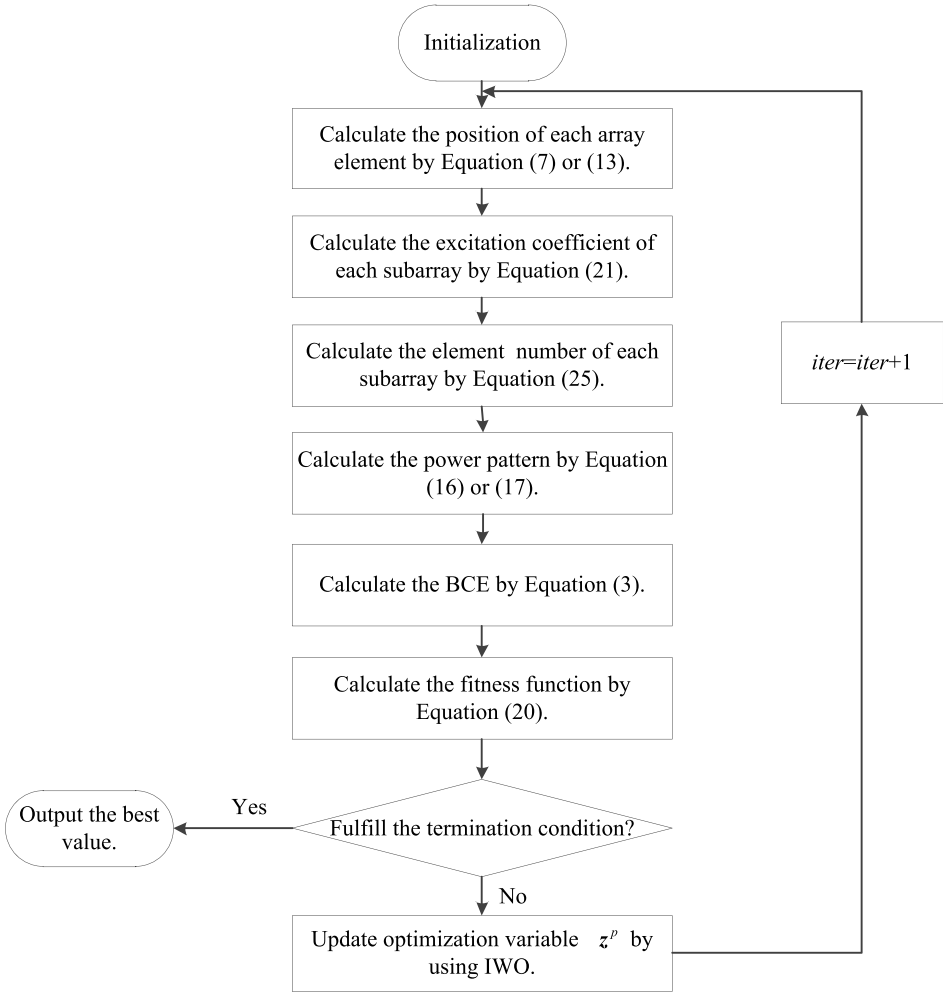

Figure 4. Optimization process of the IWO algorithm.

3.1. Example 1: The Total Number of Array Elements Is $2N = 10$

In this case, the length of the right half aperture is $L = 2.25\lambda$ (The average element spacing is 0.5λ), and the minimum element spacing is $d_e = 0.4\lambda$. The size of the receiving area ψ is achieved by changing u_0. Therefore, the BCE can be defined as

$$BCE = \frac{P_\psi}{P_\Omega} = \frac{\int_0^{u0} P(u)du}{\int_0^1 P(u)du} \tag{26}$$

The best results obtained by optimizing the element positions are shown in Table 2. It can be seen that the distances of the adjacent elements all satisfy the constraint of minimum element spacing ($2.25\lambda/0.4\lambda = 5.625$). The far-field power pattern of the antenna arrays obtained by optimizing the element positions is given by Fig. 5. Because the distribution of the array elements is symmetric, the power pattern also shows a symmetric trend.

Table 3 shows the best element positions when the antenna array is divided into several subarrays. Similarly, the minimum spacing of adjacent array elements satisfies the expected requirements. The element number and excitation coefficient of each subarray are given in Table 4. The maximum BCE and average BCE are given in Table 5. It can be seen that the BCE obtained by IWO in this paper

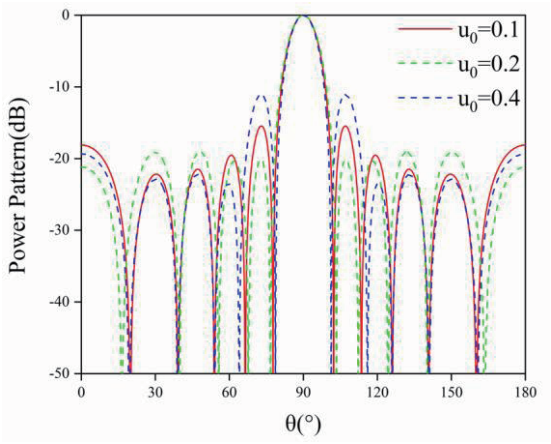

Figure 5. $2N = 10$: The far-field power pattern obtained by optimizing the element positions.

Table 2. $2N = 10$: The best position obtained by optimizing the element positions.

u	Best position
0.1	(0.615 1.658 2.927 4.117 5.625)
0.2	(0.517 1.517 2.613 3.945 5.625)
0.4	(0.803 2.088 3.232 4.232 5.625)

Table 3. $2N = 10$: The best element positions in the case of subarray division.

u	Number of subarrays	Best position
0.1	2	(0.621 1.752 3.019 4.078 5.625)
	3	(0.639 1.903 3.078 4.078 5.625)
0.2	2	(0.500 1.535 2.615 4.005 5.625)
	3	(0.500 1.582 2.608 4.013 5.625)
0.4	2	(0.621 1.752 3.019 4.149 5.625)
	3	(0.527 1.865 3.009 4.030 5.625)

is generally improved compared with the result obtained by GA in [21]. Compared with the result obtained by BSO in [21], the maximum BCE obtained by the IWO is slightly higher at $u_0 = 0.1$. When antenna array is divided into several subarrays, it is obvious that the maximum BCE and average BCE increase with the increase of the number of divided subarrays. Compared with the result obtained only by optimizing the element positions, the maximum BCE increases by 0.01%, 2.61%, and 1.46%, respectively, in the case of 2 subarrays. When the linear array is divided into 3 subarrays, the maximum BCE increases by 0.10%, 2.67%, and 1.64%, respectively.

The far-field power patterns with different numbers of subarrays are given in Fig. 6. The convergence curves of the best-fit function under different receiving areas are given in Fig. 7. It is clear that the convergence rate of IWO algorithm is quick, and it converges after about 200 iterations. The average computational time per iteration for optimizing the element position is about 6 s, and the average computational time per iteration for optimizing subarrays is about 8 s.

3.2. Example 2: Receiving Area Size Is $\mathbf{u_0 = 0.2}$

In this case, the element numbers are $2N = 10$, $2N + 1 = 15$, $2N = 20$, respectively. Accordingly, the size of right half aperture becomes $L = 2.25\lambda$, $L = 3.5\lambda$, $L = 4.75\lambda$, respectively. Other parameters are

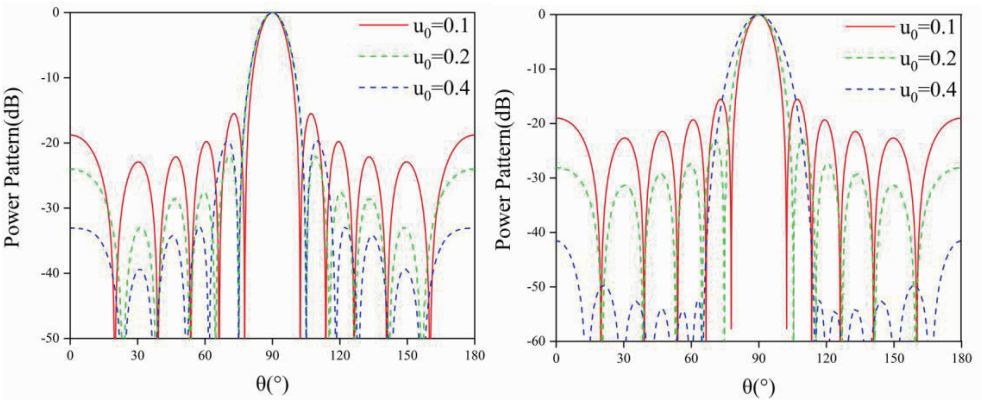

Figure 6. $2N = 10$: The far-field power pattern in different number of subarrays — (a) 2 subarrays, (b) 3 subarrays.

Table 4. $2N = 10$: The best element number and excitation coefficient of each subarray.

u	Number of subarrays	Element number of each subarray	Excitation coefficient of each subarray
0.1	2	2	1.000
		3	0.920
	3	2	1.000
		1	0.658
		2	0.904
0.2	2	4	1.000
		1	0.574
	3	1	1.000
		3	0.924
		1	0.514
0.4	2	4	1.000
		1	0.461
	3	2	1.000
		2	0.408
		1	0.136

Table 5. $2N = 10$: Maximum BCE and average BCE.

u_0	0.1		0.2		0.4	
BCE (%)	Max	Avg	Max	Avg	Max	Avg
Ref. [21], GA	79.17	79.09	95.80	95.62	98.32	98.14
Ref. [21], BSO	79.19	79.19	95.81	95.81	98.35	98.35
This paper, IWO	79.20	79.20	95.81	95.81	98.35	98.35
2 subarrays	79.21	79.21	98.42	98.35	99.81	99.81
3 subarrays	79.30	79.30	98.48	98.48	99.99	99.99

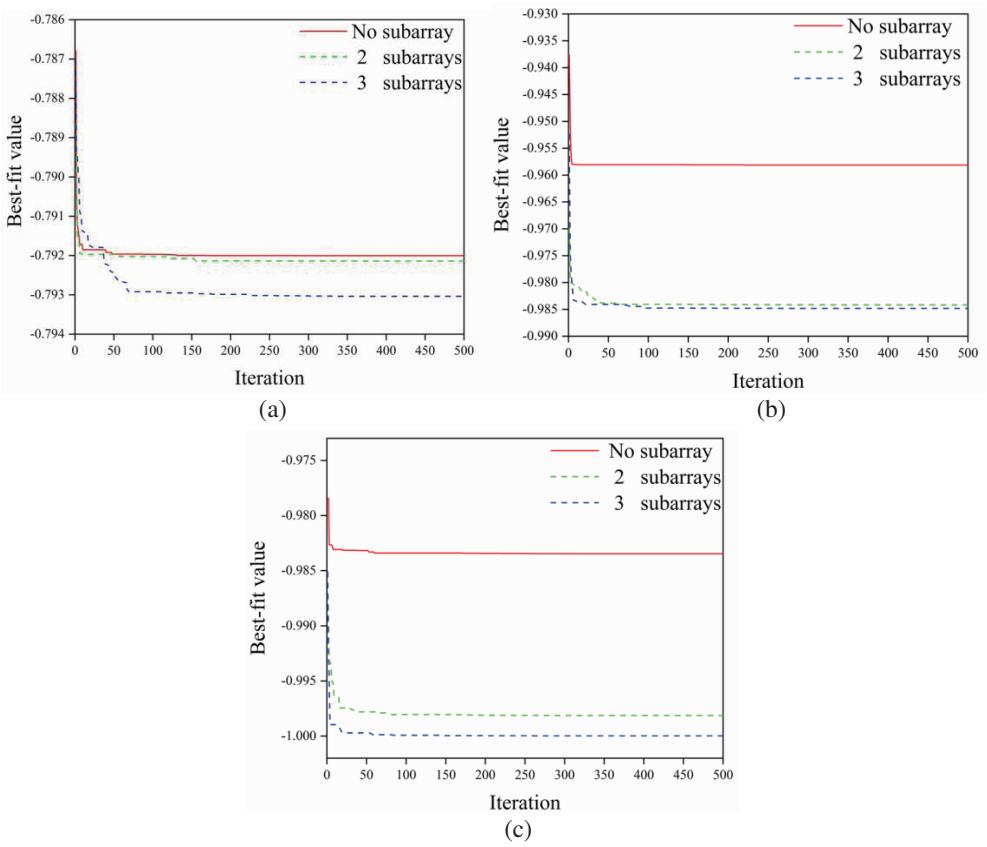

Figure 7. $2N = 10$: The best convergence curves in different receiving areas — (a) $u = 0.1$, (b)$u = 0.2$, (c)$u = 0.4$.

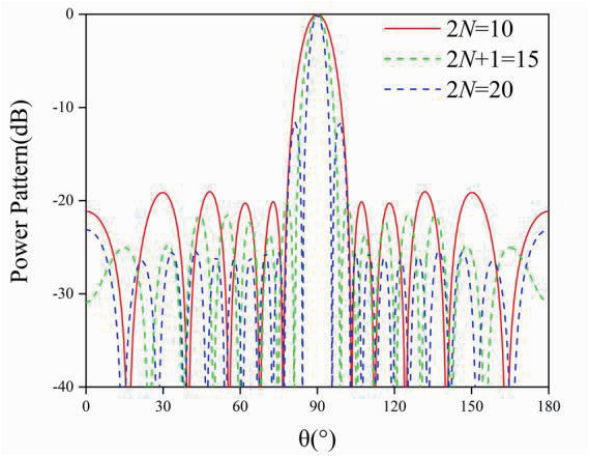

Figure 8. $u_0 = 0.2$: The far-field power pattern obtained only by optimizing the element positions.

the same as example 1.

Table 6 shows the best results obtained only by optimizing the element positions. Likewise, the distances of the adjacent elements all satisfy the constraint of minimum spacing. The far-field power pattern obtained only by optimizing the element positions is given in Fig. 8. The same conclusion that the far-field power pattern is also symmetric can be drawn.

The best element positions in the case of subarray division are shown in Table 7. Table 8 gives

Table 6. $u_0 = 0.2$: The best position obtained only by optimizing the element positions.

Number of array elements	Best position
10	(0.615 1.658 2.927 4.117 5.625)
15	(1.000 2.048 3.048 4.230 5.358 6.962 8.750)
20	(0.746 2.197 3.444 4.646 5.647 6.756 7.756 8.912 10.221 11.875)

Table 7. $u_0 = 0.2$: The best element positions in the case of subarray division.

Number of array elements	Number of subarrays	Best position
10	2	(0.500 1.535 2.615 4.005 5.625)
	3	(0.500 1.582 2.608 4.013 5.625)
15	2	(1.007 2.104 3.230 4.687 6.084 7.084 8.750)
	3	(1.000 2.090 3.223 4.707 6.395 7.603 8.750)
20	2	(0.574 1.574 2.732 3.785 5.016 6.268 7.814 9.246 10.247 11.875)
	3	(0.605 1.605 2.844 3.958 5.387 6.474 7.474 8.474 10.053 11.875)

Table 8. $u_0 = 0.2$: The best element number and excitation coefficient of each subarray.

Number of array elements	Number of subarrays	Element number of each subarray	Excitation coefficient of each subarray
10	2	4	1.000
		1	0.574
	3	1	1.000
		3	0.924
		1	0.514
15	2	4	1.000
		3	0.403
	3	4	1.000
		1	0.604
		2	0.191
20	2	7	1.000
		3	0.429
	3	5	1.000
		4	0.512
		1	0.234

the element number and excitation coefficient of each subarray. The maximum BCE and average BCE are given in Table 9. Similarly, the BCE obtained by IWO in this paper is also greater than obtained by GA in [21]. Compared with the results obtained by BSO in [21], the maximum BCE is basically the same, but the average BCE obtained by IWO is higher than BSO at $2N = 20$. It is obvious that the BCE also increases with the increase of the subarray numbers. Compared with the results obtained only by optimizing the element positions, the maximum BCE is improved by 2.61%, 2.77%, and 1.73%, respectively, only when the linear array is divided into 2 subarrays. Also, the maximum BCE increases

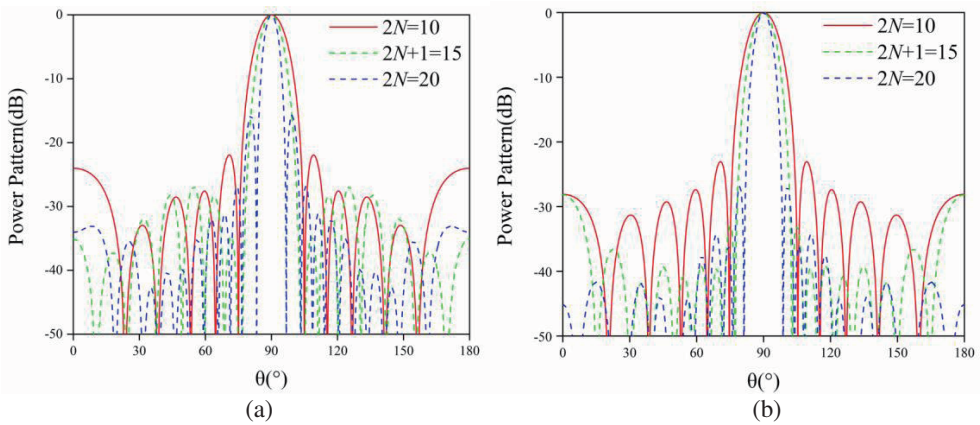

Figure 9. $u_0 = 0.2$: The far-field power pattern in different number of subarrays — (a) 2 subarrays, (b) 3 subarrays.

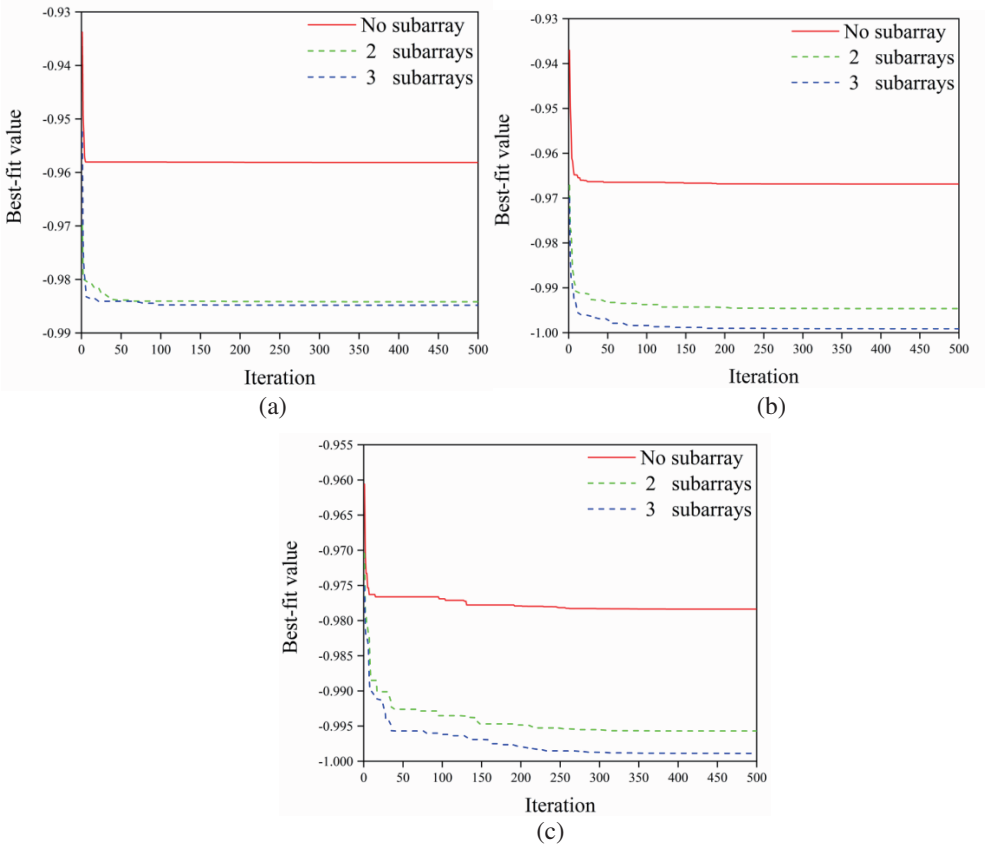

Figure 10. $u_0 = 0.2$: The best convergence curves in different number of array elements — (a) $2N = 10$, (b) $2N + 1 = 15$, (c) $2N = 20$.

by 3.67%, 3.22%, and 2.05%, respectively, in the case of 3 subarrays.

The far-field power pattern and the best-fit function convergence curves are given in Fig. 9 and Fig. 10, respectively. The difference is that the convergence rate of IWO slows down when the element number increases, and it converges completely after about 300 iterations. As the element numbers and optimization parameters increase, the average computational time per iteration for optimizing the element positions and subarrays becomes about 9 s and 11 s, respectively. Combining the above

Table 9. $u_0 = 0.2$: Maximum BCE and average BCE.

Number of array elements	10		15		20	
BCE(%)	Max	Avg	Max	Avg	Max	Avg
Ref. [21], GA	95.80	95.62	96.46	95.87	97.62	97.62
Ref. [21], BSO	95.81	95.81	96.69	96.69	97.84	97.80
This paper, IWO	95.81	95.81	96.69	96.69	97.84	97.84
2 subarrays	98.42	98.35	99.46	99.46	99.57	99.48
3 subarrays	99.48	99.48	99.91	99.90	99.89	99.85

numerical results, it can be concluded that the IWO algorithm can operate well with high efficiency and robustness.

4. CONCLUSION

In this paper, the IWO algorithm is used for comprehensive optimization of the nonuniform symmetric linear array in WPT system. The main purpose is to improve the BCE with the multi-constrained conditions. The optimization problem with different azimuth angles and different element numbers is studied. Compared with other classical literatures, the BCE obtained by IWO algorithm is improved. Additionally, the whole antenna array is divided into several subarrays, and the performance of linear array after subarray division is investigated. The element positions, excitation coefficients, and element numbers of subarrays are optimized simultaneously. The numerical results show that BCE is greatly improved. The complexity of the system is also greatly reduced in the case of subarray division. All of these prove the effectiveness and feasibility of the used algorithm and proposed method.

ACKNOWLEDGMENT

This work was supported by the National Natural Science Foundation of China (61901347) and the Shaanxi Province Science Technology Department Project (2022JM-146).

REFERENCES

1. Oliveri, G., P. Rocca, F. Viani, et al., "Latest advances and innovative solutions in antenna array synthesis for microwave wireless power transmission," *IEEE MTT-S International Microwave Workshop Series on Innovative Wireless Power Transmission: Technologies, Systems, and Applications*, 2012.
2. Massa, A., G. Oliveri, F. Viani, et al., "Array designs for long-distance wireless power transmission — State-of-the-art and innovative solutions," *Proceedings of the IEEE*, Vol. 101, No. 6, 1464–1481, 2013.
3. Morabito, A. F., R. Palmeri, V. A. Morabito, et al., "Single-surface phaseless characterization of antennas via hierarchically ordered optimizations," *IEEE Transactions on Antennas and Propagation*, Vol. 67, No. 1, 461–474, 2019.
4. Oman, H., "Electric car progress," *IEEE Aerospace & Electronic Systems Magazine*, Vol. 17, No. 6, 30–35, 2002.
5. Sasaki, S., K. Tanaka, and K. Maki, "Microwave power transmission technologies for solar power satellites," *Proceedings of the IEEE*, Vol. 101, No. 6, 1438–1447, 2013.
6. Gavan, J. and S. Tapuchi, "Microwave wireless-power transmission to high-altitude-platform systems," *URSI Radio Science Bulletin*, Vol. 334, 25–42, 2017.

7. McSpadden J. O. and J. C. Mankins, "Space solar power programs and microwave wireless power transmission technology," *IEEE Microwave Magazine*, Vol. 3, No. 4, 46–57, 2002.
8. Li, X., B. Duan, L. Song, et al., "Study of stepped amplitude distribution taper for microwave power transmission for SSPS," *IEEE Transactions on Antennas and Propagation*, Vol. 65, No. 10, 2017.
9. Li, J. and S. Chang, "Novel sparse planar array synthesis model for microwave power transmission systems with high efficiency and low cost," *Progress In Electromagnetics Research C*, Vol. 115, 245–259, 2021.
10. Mandal, S. K., G. K. Mahanti, and R. Ghatak, "Differential evolution algorithm for optimizing the conflicting parameters in time-modulated linear array antennas," *Progress In Electromagnetics Research B*, Vol. 51, 101–118, 2013.
11. Lopez, P., J. A. Rodriguez, F. Ares, and E. Moreno, "Subarray weighting for the difference patterns of monopulse antennas: Joint optimization of subarray configurations and weights," *IEEE Transactions on Antennas and Propagation*, Vol. 49, No. 11, 1606–1608, 2001.
12. Li, X., B. Duan, and L. Song, "Design of clustered planar arrays for microwave wireless power transmission," *IEEE Transactions on Antennas and Propagation*, Vol. 67, No. 1, 606–611, 2019.
13. Cui, C., Y. Jiao, L. Zhang, et al., "Synthesis of subarrayed monopluse arrays with contiguous elements using a DE algorithm," *IEEE Transactions on Antennas and Propagation*, Vol. 65, No. 8, 4340–4345, 2017.
14. Guo, H., C. Guo, and J. Ding, "Pattern synthesis of sub-arrayed monopulse planar arrays," *Electromagnetics*, Vol. 34, No. 7, 2014.
15. Guo, H., H. L. Hao, P. Song, et al., "Synthesis of planar array for wireless power transmission," *Progress In Electromagnetics Research C*, Vol. 121, 163–178, 2022.
16. Li, X., R. Li, X. Chen, et al., "Wideband frequency invariant array synthesis based on matrix singular value decomposition," *Electronics*, Vol. 10, No. 16, 2021.
17. Swist, D., A. Kumar, and G. Fettweis, "Upper bound on side lobe levels for mmimo antennas to evaluate the beam steering capability," *IEEE Communications Letters*, Vol. 25, No. 1, 2021.
18. Prasad, S., "On the index for array optimization and the discrete prolate spheroidal functions," *IEEE Transactions on Antennas & Propagation*, Vol. 30, No. 5, 1021–1023, 1982.
19. Oliveri, G., L. Poli, and A. Massa, "Maximum efficiency beam synthesis of radiating planar arrays for wireless power transmission," *IEEE Transactions on Antennas & Propagation*, Vol. 61, No. 5, 2490–2499, 2013.
20. Li, X., B. Duan, J. Zhou, et al., "Planar array synthesis for optimal microwave power transmission with multiple constraints," *IEEE Antennas and Wireless Propagation Letters*, Vol. 16, 70–73, 2017.
21. Liu, G., Q. Qin, and Q. Zhang, "Linear array synthesis for wireless power transmission based on brain storm optimization algorithm," *International Journal of Antennas and Propagation*, 2021.
22. Mehrabian, A. R. and C. Lucas, "A novel numerical optimization algorithm inspired from weed colonization," *Eco. Inform.*, Vol. 1, No. 4, 355–366, 2006.
23. Torres, T., N. Anselmi, P. Nayeri, and R. Haupt, "Low discrepancy sparse phased array antennas," *Sensors (Basel)*, Vol. 21, No. 23, 2021.
24. Keizer, W. P. M. N., "Synthesis of thinned planar circular and square arrays using density tapering," *IEEE Trans. Antennas Propag.*, Vol. 62, No. 4, 1555–1563, 2014.
25. Yang, F., S. Yang, Y. Chen, S. Qu, and J. Hu, "Synthesis of sparse antenna arrays subject to constraint on directivity via iterative convex optimization," *IEEE Antennas and Wireless Propagation Letters*, Vol. 20, No. 8, 2021.